Composites Part B 197 (2020) 108044

Contents lists available at ScienceDirect

Composites Part B

journal homepage: www.elsevier.com/locate/compositesb

New reactive rigid-rod aminated aromatic polyamide for the simultaneous strengthening and toughening of epoxy resin and carbon fiber/epoxy composites

Weitao Wang, Guodong Zhou, Boshi Yu, Mao Peng *

MOE Key Laboratory of Macromolecular Synthesis and Functionalization, Department of Polymer Science and Engineering, Zhejiang University, Hangzhou, 310027, China

ARTICLE INFO

Keywords:
Rigid-rod polymer
Reinforcement
Toughening
Composites
CFRP

ABSTRACT

In recent years, nanomaterial reinforced composites have been extensively studied, however, research on molecular composites, i.e. composites reinforced by rigid-rod macromolecules of large aspect ratio and superior mechanical properties, is still rare. In this study, we report that when a new organosoluble rigid-rod aromatic polyamide, poly(p-aminophenylene terephthalamide) (NH_2-PPTA), is used as a reinforcing agent of epoxy resin, it is dispersed in epoxy at molecular level at low contents but forms nanorod- or nanofiber-like aggregates in the matrices at higher contents, thereby transforming the molecular composite into a nanocomposite. The reactive amino side groups can not only improve the solubility of NH_2-PPTA in epoxy but also participate in the curing reaction, which leads to the formation of covalent bonds between NH_2-PPTA and the matrix. At a content as low as 0.7 wt%, NH_2-PPTA remarkably improves the strength and toughness of epoxy resin with a tensile strength of 100.7 ± 5.3 MPa and tensile toughness of 2860 ± 316 kJ/m^3, which are increased by ~74% and ~118%, respectively. The strengthening and toughening effects are comparable to those provided by graphene oxide, and are higher than by many other previously reported inorganic nanofillers. Moreover, NH_2-PPTA also significantly improves the mechanical properties of carbon fiber (CF)/epoxy composites. Flexural strength, total fracture energy and interlayer shear strength are increased by ~9%, ~67% and~27%, respectively. This is the first report on the transition of molecular composite to nanocomposite and the effective strengthening and toughening of epoxy resin and CF reinforced composites by NH_2-PPTA.

1. Introduction

In recent years, influence of nanomaterials, such as carbonaceous and other inorganic nanofibers and nanosheets, on the mechanical properties of polymeric composites has been extensively studied. However, surface modification of these nanomaterials is relatively complicated and it is difficult to disperse the nanomaterials uniformly in polymer matrices. On the other hand, due to the unique molecular morphology, excellent mechanical and thermal properties, rigid-rod macromolecules have been suggested to be used as the reinforcing agent of flexible-chain polymers [1]. The molecular composites can show remarkably improved mechanical properties, low density, good processability and wide range of applications, compared with traditional composites filled with inorganic nanomaterials [2–4]. However, only when rigid-rod polymers are uniformly dispersed in the polymer matrix can molecular composites show excellent reinforcement effects. Flory [5] studied the dispersion of rigid and flexible macromolecular chains in solvents by using the nematic liquid crystal lattice model and predicted that when rigid and flexible polymers are blended or dissolved in a solvent, incompatibility or phase separation would occur as a result of the small mixing entropy and the positive mixing enthalpy in the mixing process. In order to solve this problem, researchers had introduced ionic interactions [6–8], acid-base interactions [9–11] and hydrogen bonding interactions [12,13] to reduce the agglomeration of rigid polymers. In our previous study, molecular composites of poly(*p*-sulfophenylene terephthalamide) (sPPTA) reinforced poly(vinyl alcohol) (PVA) were prepared, which exhibit greatly improved compatibility and reinforcement effect due to the hydrogen bond interaction between the sulfonic acid side groups of sPPTA and the hydroxyl groups of PVA [14].

Epoxy resin is widely used in various fields as an advanced material

* Corresponding author.
E-mail address: pengmao@zju.edu.cn (M. Peng).

https://doi.org/10.1016/j.compositesb.2020.108044
Received 13 January 2020; Received in revised form 5 April 2020; Accepted 6 April 2020
Available online 15 May 2020
1359-8368/© 2020 Elsevier Ltd. All rights reserved.

because of low curing shrinkage, good physical, mechanical and insulation properties, corrosion resistance and bonding strength in thermosetting polymer materials [15–18]. Many studies have focused on the modification of epoxy by nanofillers, such as carbon nanotubes (CNTs) [19–24], vapor grown carbon fibers (VGCFs) [25,26], nanoclay [27–29], alumina platelets [30,31], graphene oxide (GO) and its derivatives [32–40], because of their high strength and modulus [41]. These nanofillers have also been demonstrated to be very useful in carbon fiber reinforced polymers (CFRPs) as the secondary reinforcement [42–48]. However, surface modification of nanomaterials is usually required for their uniform dispersion in the matrices, which is relatively complex and time-consuming [49–52]. sPPTA has also been demonstrated to be an effective reinforcing and toughening agent for epoxy resins, however, significantly reduces the glass transition temperature (T_g) of epoxy resin, thus reducing the heat resistance of the composites.

Here, we report the synthesis of a new aminated aromatic polyamide and its reinforcing and toughening effect on epoxy resin and epoxy-based CFRPs. Poly(p-nitrophenylene terephthalamide) (NO_2-PPTA) was synthesized by low-temperature solution polycondensation, and then poly (p-aminophenylene terephthalamide) (NH_2-PPTA) was obtained by hydrogen-reduction. Because of the introduction of amino groups, the solubility of NH_2-PPTA in organic solvents was significantly improved compared with that of Kevlar. NH_2-PPTA was then added as a reinforcing agent to triglycidyl-p-aminophenol (TGPAP). Chemical structure of NH_2-PPTA was characterized and its influence on the microstructure, thermal stability and mechanical properties of epoxy resin were investigated. Furthermore, influence of NH_2-PPTA on the mechanical properties of epoxy-based CFRPs was also reported.

2. Experiments

2.1. Materials

Terephthaloyl chloride (TPC) and 2-nitro-1, 4-phenylenediamine was supplied by J&K Chemical Ltd. (Shanghai, China). 2-Nitro-1, 4-phenylenediamine was used after purification by recrystallization. N, *N*-Dimethylacetamide (DMAc), lithium chloride (LiCl), palladium-carbon catalyst (Pd/C), calcium hydride (CaH_2), ethanol and pyridine were purchased from Sinopharm (Shanghai, China). DMAc and pyridine were dehydrated by CaH_2 for few days. Epoxy resin TGPAP was obtained from Shanghai Huayi Resins Co., Ltd. The curing agent of epoxy resin used was 3,5-Dimethylthio-2,4-toluenediamine (DMTDA) for all the composites, which was supplied by Johnson Chemicals Co. (Haining, China). Dimethyl sulfoxide-d6 (DMSO-d_6) for ^{1}H NMR was purchased from Cambridge Isotope Laboratories, Inc. Unidirectional T700 carbon fabrics were supplied by Toray Industries, Inc., Japan.

2.2. Synthesis of NO_2-PPTA and of NH_2-PPTA

Scheme 1 shows the synthesis of NO_2-PPTA and NH_2-PPTA. NO_2-PPTA was synthesized by low-temperature solution polycondensation under the conditions similar to those in the literature [53–55]. 36.75 g of 2-nitro-1,4-phenylenediamine and 12 g of LiCl were dissolved in DMAc (600 mL) and pyridine (60 mL) in a three-necked flask. After the solution was cooled to 0 °C and purged with nitrogen for half an hour, 52.79 g of TPC powder was directly added to the flask under magnetic stirring. The solution was further stirred for about 10 min until gelation appeared and then heated to 80 °C for an hour to complete the polycondensation. The final opaque solution was then poured into deionized water and the precipitate was separated by filtration. The precipitate was washed twice with deionized water and ethanol, respectively, and then dried at 80 °C to obtain a yellow powder. The molecular weight of NO_2-PPTA was measured by gel permeation chromatography (GPC) using DMF as the solvent. The number-average and weight-average molecular weights are about 22,307 and 26,262 g mol^{-1}, respectively. A solution of NO_2-PPTA (20 g), 10% Pd/C (0.2 g), and LiCl (10 g) in DMAc (500 mL) was heated at 108 °C for 12 h and 24 h, respectively, under a hydrogen atmosphere. After cooling and removing the Pd/C powder from the solution by vacuum filtration, the polymer solution was poured into deionized water. The precipitate in the form of a brown powder was separated by filtration, first washed with deionized water, then washed thoroughly with ethanol, and then dried under vacuum at 80 °C overnight.

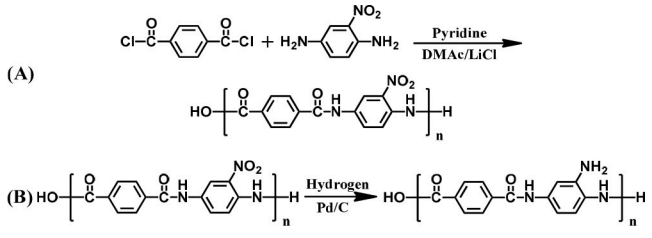

Scheme 1. (A) Synthesis of NO_2-PPTA and (B) preparation of NH_2-PPTA.

2.3. Preparation of NH_2-PPTA/epoxy composites and CF/NH_2-PPTA/epoxy multi-scale composites

The NH_2-PPTA/epoxy composites were fabricated by casting molding. NH_2-PPTA was first dissolved in DMAc. The solution was poured into TGPAP at 80 °C and magnetically stirred to homogenize the mixture. The mixture was washed by deionized water and heated at 130–150 °C to remove deionized water. The curing agent dimethyl sulfide toluene diamine (DMTDA) was added into the mixture. The mass ratio of epoxy to DMTDA was 2:1 for all the samples. The viscous NH_2-PPTA/epoxy mixtures were heated at 80 °C under vacuum. After all air bubbles have been removed, the mixtures were poured into a mold, heated at 120 °C and 150 °C for half an hour, respectively, then heated at 170 °C for about two and a half hours, and finally heated at 200 °C for 1 h. The NH_2-PPTA content in the composites was between 0.1 and 1.3 wt %.

The preparation method of CF/NH_2-PPTA/epoxy composite is hand lay-up and high temperature hot-pressing. The NH_2-PPTA/TGPAP mixtures with various NH_2-PPTA contents were mixed with DMTDA and then coated onto rectangular CF sheets with a length of 17 cm and a width of 10 cm. Ten layers of the coated unidirectional CF sheets were then parallelly stacked, degassed in an vacuum oven at 80 °C for one hour and then transferred into a hot press for curing. The composites were first heated at 120 °C and 150 °C for half an hour, respectively, pressurized to 6 MPa and then heated at 170 °C for 2.5 h, heated at 200 °C for one hour, and then cooled to ambient temperature and pressure.

2.4. Characterization

The molecular weight of NO_2-PPTA is measured by GPC (Wyatt DAWN-DSP, USA). Fourier transform infrared (FTIR) spectra were measured with KBr pellets in a Bruker Vector-22 FTIR spectrophotometer (Germany). ^{1}H NMR spectra were recorded on a Varian Unity Inovaspectrometer (Advance2B, Bruker, Germany) operated at 500 MHz, using DMSO-d_6 as the solvent. Dispersion of NH_2-PPTA in epoxy matrix was observed by transmission electron microscopy (TEM) using a 80 kV JEM-1200EX microscope (JEOL Ltd., Japan). Wide-angle X-ray diffraction (XRD) measurements were performed to study the crystalline structure of the NH_2-PPTA/epoxy composites on a PANalytical X'Pert PRO MPD X-ray diffractometer (The Netherlands). A tensile testing machine (Shenzhen SUNS Technology Co., Ltd., China) was used to measure the tensile properties of the NH_2-PPTA/epoxy composites under ambient conditions according to ASTM D638-03. Dumbbell samples (60 × 20 × 4 mm^3) with a gauge length of 25 mm were used. The tensile speed was 1.0 mm/min. A RG-3010 electronic universal testing machine (Reger, China) was employed to measure the flexural

properties of the composites under ambient conditions. According to the ASTM D-790 standard, the specimen span was 32 mm and the cross-head speed was 2.0 mm/min. An impact test machine Model ZBC1400-2 (Shenzhen SANS, China) was used to measure the notched Izod impact strength, according to ASTM D256. The dimension of the specimens was 80 × 10 × 4 mm^3 with a V-shape notch of 2 mm. For the CF/NH_2-PPTA/epoxy composites, the flexural properties were determined according to ASTM D-790 with a span length of 64 mm and a crosshead velocity of 2.0 mm/min. ASTM D2344 standard was used to determine ILSS using a span length of 8 mm and a cross-head velocity of 1.0 mm/min. The size of the specimens was 80 × 15 × 2 mm^3. The test of all the above mechanical properties was under displacement control conditions and each data is the average of six sample data. Scanning electron microscopy (SEM) images were used to observe the fracture surfaces of samples on a Hitachi S-4800 FESEM. The thermal stability of the composites was characterized by thermogravimetric (TG) analysis in nitrogen on a SDT Q600 thermal analyzer (TA, USA) at a heating rate of 10 °C/min from 50 °C to 950 °C. A Q800 Dynamic Mechanical Analyzer (TA Instruments, USA) was used to perform the dynamic mechanical analysis (DMA) of the NH_2-PPTA/epoxy composites. The experiments were carried out in a tensile mode under a nitrogen atmosphere. The heating rate was 3 °C/min, the frequency was 1 Hz and the size of the rectangular specimen strips is 60 × 10 × 2 mm^3.

3. Results and discussions

3.1. Characterization of NH_2-PPTA

FTIR was used to characterize the hydrogenation reduction process of NO_2-PPTA. The FTIR curve of NO_2-PPTA (see Fig. 1) displays a significant C═O stretching vibration peak of amide at 1673 cm^{-1} [56–58], which red-shifts in the FTIR curves of NH_2-PPTA to 1658, 1658 and 1644 cm^{-1} because of the conjugation effect of the amino side groups in NH_2-PPTA [59]. The peak intensity of N═O stretching vibration of nitro side groups at 1507 cm^{-1} decreases obviously with the increase of reduction time and slightly red-shifts, demonstrating the occurrence of the hydrogenation reduction. NH_2-PPTA exhibits remarkably improved solubility compared with NO_2-PPTA. In a solvent of DMAc and lithium chloride (LiCl), NH_2-PPTA forms a uniformly, stable and transparent solution at a concentration below 8%, and forms an anisotropic liquid crystal phase at the concentration between 8% and 13%, and forms a gel when the concentration exceeds 13%.

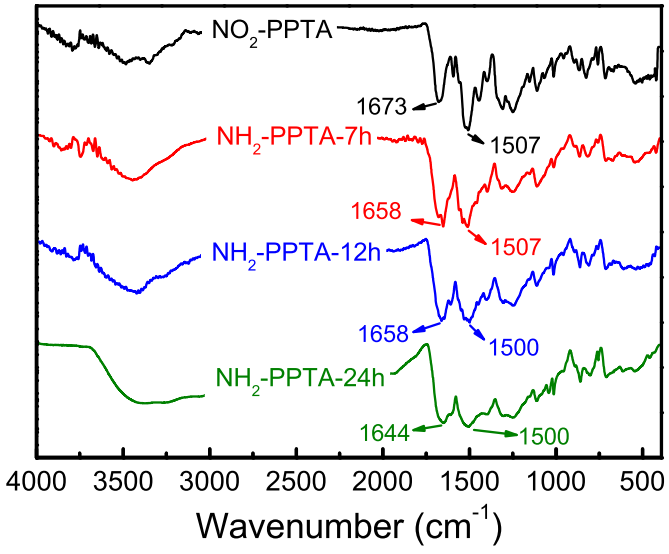

Fig. 1. FTIR spectra of NO_2-PPTA, NH_2-PPTA-7h, NH_2-PPTA-12h and NH_2-PPTA-24h.

The TG curves of commercial aramid fiber (Kevlar), NO_2-PPTA and NH_2-PPTA and corresponding differential TG (dTG) curves are presented in Fig. 2. The weight loss in the temperature range of 50–200 °C should be caused by the loss of water absorbed in the samples. For the aramid fiber, there is only one decomposition peak temperature at 578 °C. With the introduction of nitro side groups and amino side groups, the decomposition temperature obviously shifts to lower temperatures. As shown in Fig. 2(B), for NO_2-PPTA, noticeable drop in weight at 407 °C can be ascribed to the departure of nitro side groups. As the reaction time for hydrogenation reduction increases, the residual weight increases significantly, indicating that the amount of amino groups attached to the rigid macromolecular backbone increases with the reduction time. Moreover, for NH_2-PPTA, a new decomposition peak appears at 306 °C due to the lower thermal stability of amino side groups, and when the reaction time for hydrogenation reduction is 12 and 24 h, the decomposition peak at 407 °C becomes much weaker, indicating that most nitro side groups have been converted to amino side groups, which is in good agreement with the above-mentioned FTIR result.

The molecular structure of NO_2-PPTA and NH_2-PPTA wasfurther characterized by ^1H NMR spectra (see Fig. 3). The existence of a chemical shift at ~11.81 ppm of amide group confirms the formation of polyamide. The resonances for the aromatic protons of the nitro-substituted aromatic ring occurred at 8.76 ppm, 8.36 ppm, 8.24 ppm, 7.94 ppm, 7.76 ppm. It is noted that the resonance for the protons of the

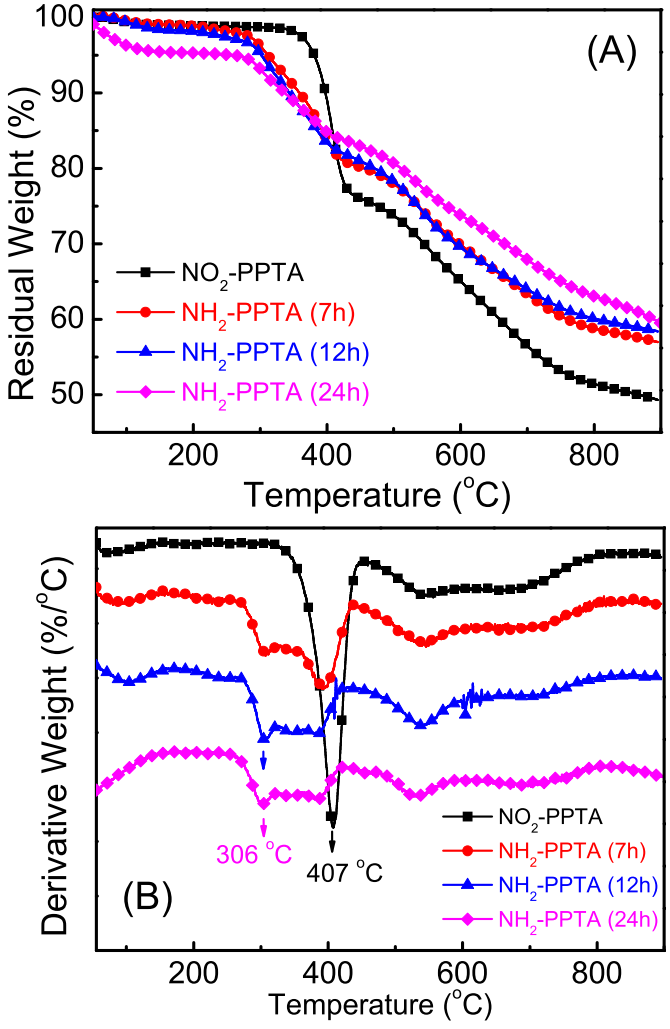

Fig. 2. (A) TG curves and (B) dTG curves of aramid fiber, NO_2-PPTA and NH_2-PPTA.

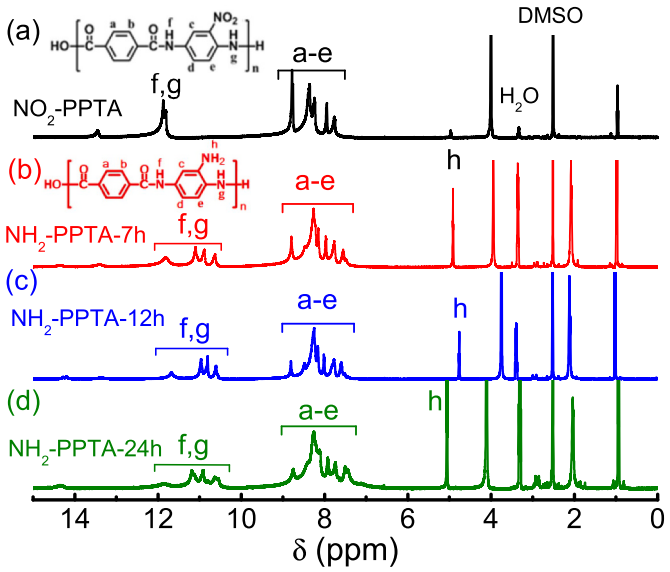

Fig. 3. ^{1}H NMR spectra of (a) NO_2-PPTA and NH_2-PPTA hydrogenated for (b)7 h, (c) 12 h, and (d) 24 h.

amino group appeared at ~4.9 ppm after the hydrogenation reduction of NO_2-PPTA, confirming the conversion of nitro to amino side groups. Moreover, with the hydrogenation reduction of NO_2-PPTA, the band at 11.81 ppm for amide groups (–CONH–) decrease significantly and new bands at 10.40–11.40 ppm appear, as the result of the conjugative effect of the amino side groups. The resonance at 8.76 ppm for the aromatic protons of the nitro-substituted aromatic ring decrease remarkably and other resonances between 7.76 ppm and 8.36 ppm also shift to some extent, as the result of conversion of nitro to amino side groups. The yields of the hydrogenation reduction reaction are obtained by calculating the ratio of the integral area of amido bond signals at ~11.81 ppm to the integral area of the signals in the range of 10–12 ppm, which are approximately 69%, 82% and 91% for the reduction for 7h, 12 h and 24 h, respectively.

3.2. Dispersion of NH_2-PPTA in epoxy

The microstructure of the NH_2-PPTA/epoxy composites was investigated by TEM, as shown in Fig. 4. For neat epoxy, 0.1 wt%–NH_2–PPTA/epoxy and 0.3 wt%–NH_2–PPTA/epoxy, the TEM images are featureless, suggesting that the samples are homogeneous and the NH_2-PPTA molecules disperse uniformly in the matrix. For 0.5 wt%–NH_2–PPTA/epoxy, some dark inclusions become observable in the samples, some of which are nanorod-like or nanofiber-like as denoted by the arrow. The dark domains are more obvious with the increase of NH_2-PPTA content, which indicates the occurrence of aggregation and/or microphase separation [60]. The high magnification TEM image in Fig. S1 clearly shows the existence of nanorod-like or nanofiber-like aggregates with a diameter of less than 40 nm in the 0.9 wt%–NH_2–PPTA/epoxy composites. Previous studies have demonstrated that epoxy resins and thermoplastics undergo phase separation due to their incompatibility, resulting in a sea-island or bicontinuous two-phase structure [61,62]. For some polyamides that can react with the matrix, phase separation can be greatly suppressed, therefore, the polyamides disperse homogeneously in the matrix [63]. As is well known, the amino side groups of NH_2-PPTA are reactive with epoxy resin, which explains why the NH_2-PPTA/epoxy composites are optically transparent and homogeneous at relatively low NH_2-PPTA contents. The NH_2-PPTA molecules aggregate at relatively high content, possibly because of the strong intermolecular attraction between the main chains of the NH_2-PPTA macromolecules, thus form nanometer-sized rods or fibers in the matrix due to their rigid rod-like macromolecular structure.

Fig. 5 presents the XRD patterns of NH_2-PPTA, neat epoxy and NH_2-PPTA/epoxy composites with various amounts of NH_2-PPTA contents. The two diffraction peaks at $2\theta = 7.4^\circ$ and 19.8° are broad and weak, corresponding to the amorphous thermosetting epoxy resin. NH_2-PPTA show two peaks centered at $2\theta = 10.0^\circ$ and 23.8°, confirming that NH_2-PPTA has a crystalline structure due to its rigid molecular structure. The patterns of NH_2-PPTA/epoxy composites are similar to that of neat epoxy and the diffraction peaks of neat NH_2-PPTA can not be observed. This suggests that most NH_2-PPTA macromolecules disperse in molecular-level in the epoxy matrix. The dark inclusions observed in TEM cannot be the simple aggregates of neat NH_2-PPTA but the mixture

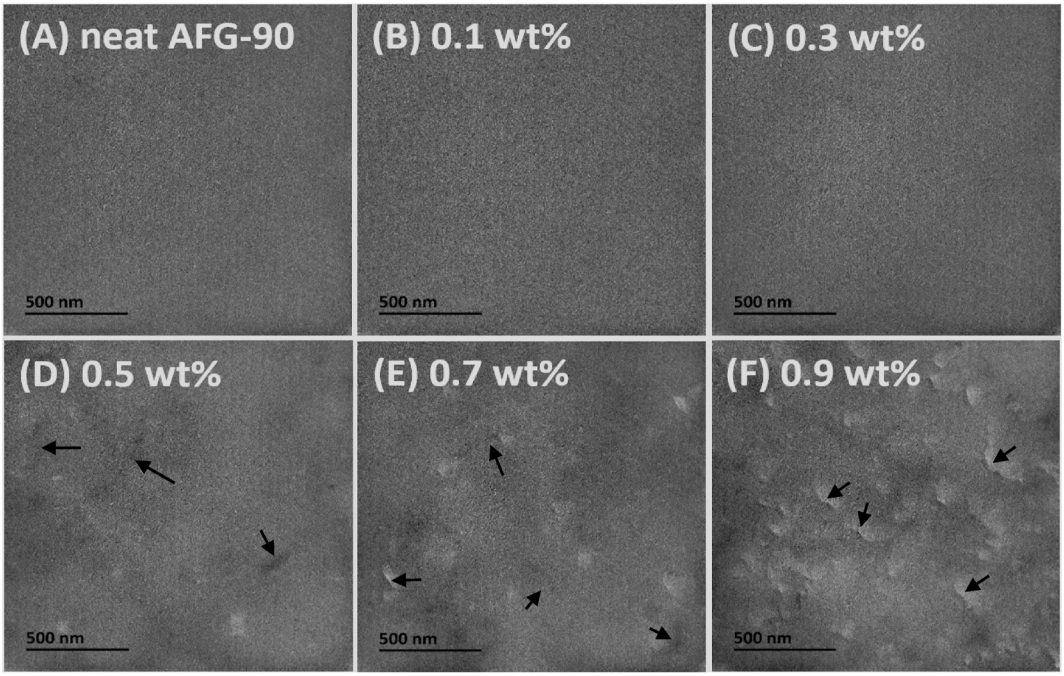

Fig. 4. TEM images for (A) neat epoxy resin, (B) 0.1 wt% (C) 0.3 wt% (D) 0.5 wt% (E) 0.7 wt% and (F) 0.9 wt%–NH_2–PPTA/epoxy.

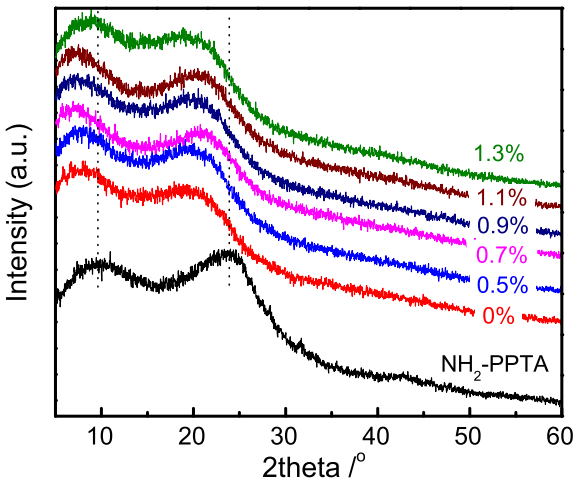

Fig. 5. XRD patterns of NH_2-PPTA, neat epoxy and NH_2-PPTA/epoxy composites.

of NH_2-PPTA and epoxy molecules with relatively high NH_2-PPTA contents that are not fully dispersed in the matrix. Any neat NH_2-PPTA aggregates formed in the matrix can only be composed of few NH2-PPTA macromolecules; otherwise, the diffraction peak of neat NH_2-PPTA should be able to be identified.

3.3. Mechanical properties of NH_2-PPTA/epoxy composites

The mechanical properties of the neat epoxy and NH_2-PPTA/epoxy composites are presented in Fig. 6. The tensile properties including tensile strength (σ_t) and Young's modulus (E_t), elongation at break (ε) and tensile toughness (K), the flexural properties including flexural strength (σ_f), flexural modulus (E_f) and flexural toughness (A), and notched impact strength (IS) of neat epoxy and NH_2-PPTA/epoxy composites are summarized in Table S1. Addition of low content of NH_2-PPTA remarkably increases the tensile and flexural properties of NH_2-PPTA/epoxy composites. 0.7 wt%–NH_2–PPTA/epoxy shows a tensile strength of 100.7 ± 5.3 MPa, ~74% higher than that of pure epoxy resin (57.8 ± 6.0 MPa), confirming that NH_2-PPTA is very effective as a molecular reinforcing agent for epoxy resin. The tensile strength is not further improved when the content of NH_2-PPTA is further increased (≤1.3 wt%), which may be due to the aggregation of NH_2-PPTA macromolecules in epoxy at higher contents, as shown by TEM images in Fig. 4. However, it is interesting that the NH_2-PPTA/epoxy composites still remain much higher tensile strengths than pure epoxy resin. What needs to be emphasized is that NH_2-PPTA also remarkably increases the toughness of the composites. The maximum elongation at break in increased to 5.6 ± 0.3% and the tensile toughness in increased to 2860 ± 316 kJ/m^3, which are ~30% and ~131% higher than those of pure epoxy resin, respectively. When the content of NH_2-PPTA is 0.5 wt%, Young's modulus is increased to 2.70 ± 0.13 GPa, which is increased by ~34% compared with that of neat epoxy resin. Fig. 6(C) and (D) present the flexural properties, which show that the flexural strength is also improved and reaches a maximum value of 179.2 ± 0.9 MPa for 0.9 wt %–NH_2–PPTA/epoxy, which is increased by ~41%. The flexural toughness (A) reaches the peak value of 0.56 ± 0.03 J for 0.9 wt%–NH_2–PPTA/epoxy, which is increased by ~143%. The flexural modulus of the composites is not increased, possibly due to the relative low modulus of NH_2-PPTA compared with that of inorganic nanofillers. The notched Izod impact strength of 0.7 wt%–NH_2–PPTA/AFG-90 is also increased by ~14%, confirming that the toughness of epoxy is also increased by very small amount of NH_2-PPTA.

Previous studies have demonstrated that many nanofillers can improve the mechanical properties of epoxy resins. In Table S2, the increase of the mechanical properties of epoxy resins by previously reported nanofillers is summarized. It is noted that the increase of the mechanical properties of NH_2-PPTA/epoxy composites is comparable

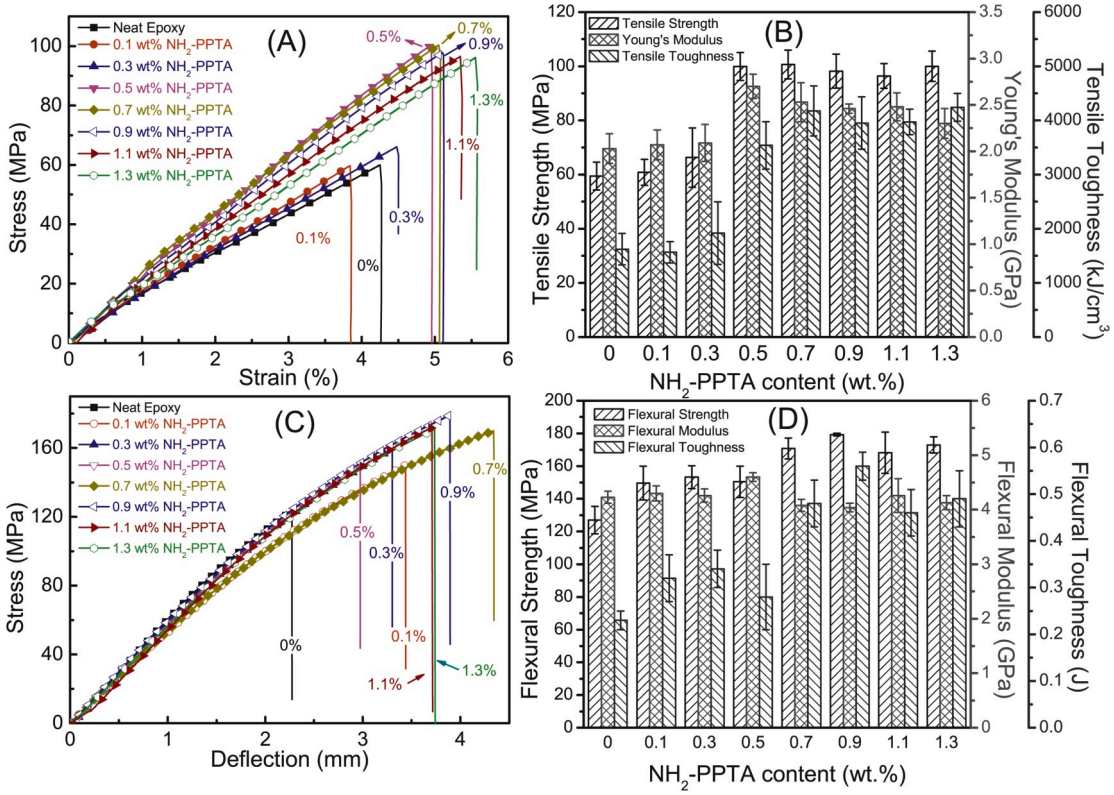

Fig. 6. (A) Stress-strain curves and (B) tensile properties; (C) stress-deflection curves and (D) flexural properties.

with that provided by GO [36,64,65], and is superior to those of provided by many other previously reported nanofillers. GO is a type of widely studied nanofiller with remarkable reinforcing effect, however, it has disadvantages of easy aggregation, low compatibility with polymers and high cost. In contrast, the synthesis and hydrogenation reduction of NO_2-PPTA is relatively simple and easier to scale-up, and the product NH_2-PPTA can be dissolved in some organic solvents, such as DMF and DMAc, which facilitates its convenient blending with epoxy. The strong interaction between NH_2-PPTA and epoxy resin and formation of chemical bonds between them ensure effective stress transfer to the reinforcing phase. NH_2-PPTA also significantly improves the flexural toughness and elongation at break of the composites. These results confirm that both the strength and toughness of epoxy resins can be remarkably increased by NH_2-PPTA.

The morphology of both the tensile and flexural fracture surfaces were observed by SEM to further analyze the reinforcing and toughening effect of NH_2-PPTA on epoxy, as shown in Fig. 7, Figs. S2 and S3. For neat epoxy resin, the fracture surfaces demonstrate the typical features of brittle polymers, where "river-like" fracture patterns with long and parallel ripples and the smooth regions between the ripples indicate that cracks propagate rapidly and are seldom deflected during the crack development. However, as shown in Figs. S2 and S3, the fracture surfaces of the NH_2-PPTA/epoxy composites with only 0.1 and 0.3 wt% of NH_2-PPTA become rougher and more cracks and ripples emerge, indicating that the propagating crack fronts are hindered and extend in different directions, which can consume more energy and thus improve the toughness of the NH_2-PPTA/epoxy composites [66]. When the NH_2-PPTA content is above 0.7 wt%, the fracture surfaces become extremely rough and a large amount of distorted and randomly oriented small cracks are observed. Many submicrometer-sized protruding particles, small cavities, fine fibers and ripples can be observed on the fracture surfaces of composites with high NH_2-PPTA contents, which results in more energy consumption during fracture and better toughness of the composites. The high magnification SEM image in Fig. 8 shows that there are a large amount of small irregular particles with diameter less than 200 nm on the fracture surfaces of 0.5 wt%–NH_2–PPTA/epoxy composites. For 0.9 wt%–NH_2–PPTA/epoxy composites, rod- or fiber-like particles protruding on the fracture surfaces

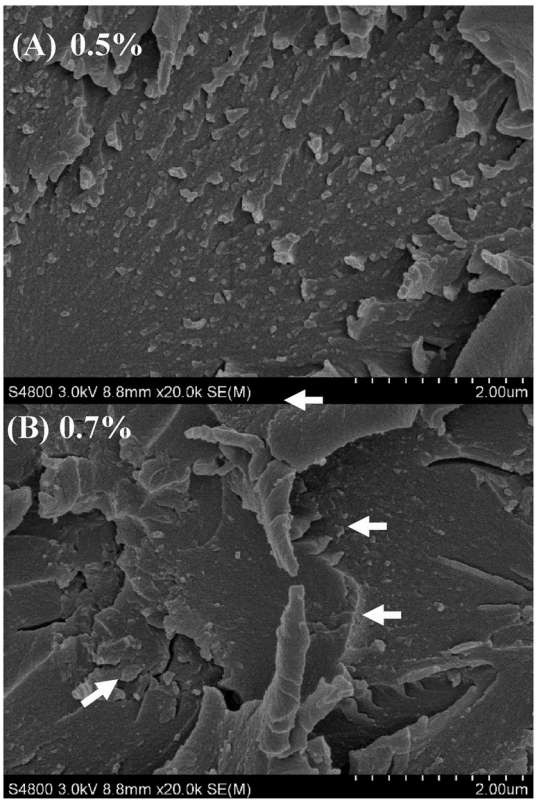

Fig. 8. High magnification SEM images of NH_2-PPTA/epoxy composites with 0.5 wt% and 0.7 wt% of NH_2-PPTA.

are observed, which are of several hundred nanometers in diameter. This result is also in consistence with the TEM result showing the existence of nanorod- or nanofiber-like aggregates of several tens of nanometers in diameter in the composites. However, the size of rod- or fiber-like particles on the fracture surfaces is about one order of

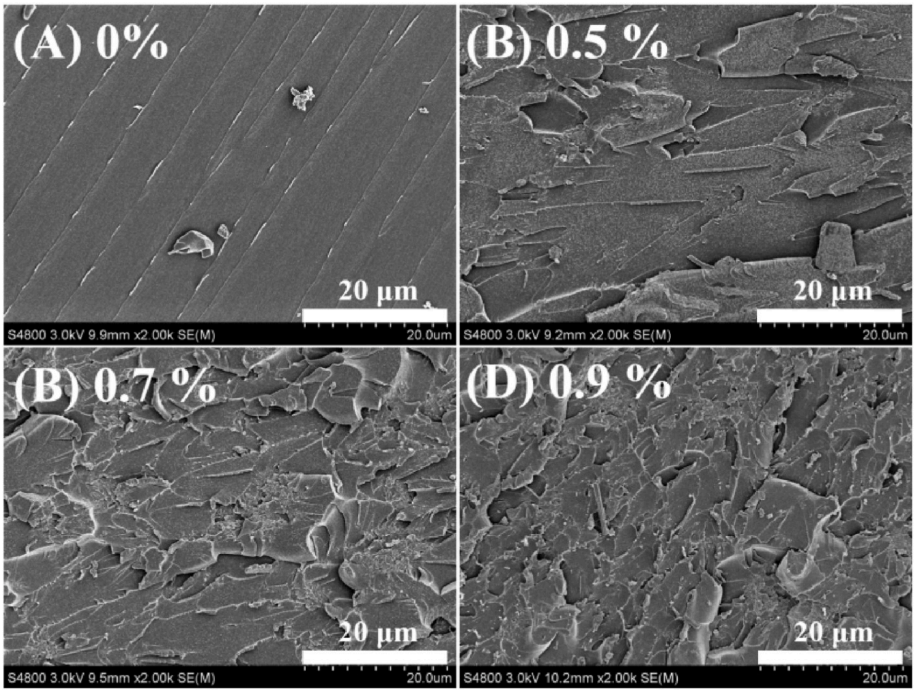

Fig. 7. SEM images of neat epoxy resin and NH_2-PPTA/epoxy composites.

magnitude larger than that of the nanorod- or nanofiber-like aggregates observed by TEM, indicating that the aggregates are encapsulated by matrix resin when being pulled out of the fracture surfaces, due to the strong filler-matrix interfacial interaction.

Basing on above experimental results, the mechanism for the strengthening and toughening of epoxy resin by NH_2-PPTA can be summarized as follows. With the increase of NH_2-PPTA contents, the molecular composites transfer to nanocomposites. Therefore, the mechanism for the strengthening and toughening is related to the content of NH_2-PPTA. At low contents, NH_2-PPTA disperses at the molecular level in the matrix. As a rigid-rod aromatic polymer with extended molecular chains, NH_2-PPTA is superior to amorphous and flexible polymers in mechanical properties, because theoretical research has shown that the energy required for the deformation of molecular chain caused by bond angle bending is ten times of the energy required for bond angle rotation, while the energy required for bond extension can reach 100 times of the rotation of bond angle [67]. On the other hand, the amino side groups of NH_2-PPTA can react with epoxy matrix, thereby facilitating the transfer of stress from the matrix to NH_2-PPTA. Therefore, the energy required for deformation and failure of NH_2-PPTA/epoxy composites is much higher. When the content of NH_2-PPTA is high, NH_2-PPTA aggregates to form nanorods or nanofibers. The mechanism for the strengthening and toughening should be similar to that of nanocomposites. At higher NH_2-PPTA content, the aggregation becomes more significant, thereby reducing the modification effect.

The influence of NH_2-PPTA on the dynamic mechanical properties of epoxy was investigated with DMA. The storage modulus (E′) and loss tangent (tan δ) as the functions of temperature are shown in Fig. 9. The storage modulus of 0.1–0.5 wt%–NH_2–PPTA/epoxy composites almost is almost the same with that of neat epoxy. However, E′ of 0.7 and 0.9 wt %–NH_2–PPTA/epoxy composites increases at temperatures below 150 °C. The tan δ curves show that addition of NH_2-PPTA does not lead to apparent shifting of T_g peaks to low temperatures. In contrast, previous studies have shown that graphene oxide, carboxylated carbon nanotubes and sulfonated aromatic polyamide decrease the T_g values of epoxy greatly by more than 30 °C because the carboxyl and sulfonic acid group change the stoichiometric ratio between epoxy resin and the curing agent, thus reducing the crosslinking density. In contrast, the amount of NH_2-PPTA added in epoxy is rather low and the small amount of additional amino group of NH_2-PPTA does not significantly reduce the crosslinking density of epoxy, thus the T_g values and heat resistance of NH_2-PPTA/epoxy resin are not reduced.

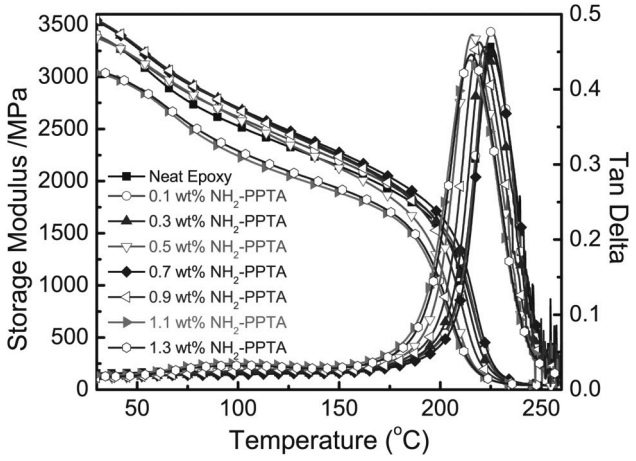

Fig. 9. Storage modulus (E′) and tan δ curves.

3.4. Mechanical properties of CF/NH_2-PPTA/epoxy composites

As is well known, continuous fiber reinforced composites have the disadvantage of low interfacial strength and brittleness of the matrix [68]. As aforementioned, the mechanical properties of NH_2-PPTA/epoxy composites are greatly increased, therefore, it is reasonable to speculate that NH_2-PPTA can also be used for the modification of the CF/NH_2-PPTA/epoxy composites [69]. Flexural strength (σ_f) and modulus (E_f) of the CF/NH_2-PPTA/epoxy composites were then measured by three-point bending test, and interlaminar shear strength (ILSS) was measured by short-beam shear test. Moreover, the toughness of the CF reinforced composites was characterized by total energy (E_{tot}), i.e. the sum of the energy dissipated during fracture, which was calculated by the integral of the load-deflection curve in the range from zero to maximum load [70]. The flexural properties and the ILSS values of the CF reinforced epoxy composites are presented in Fig. 10 and Table S3. It can be found that NH_2-PPTA not only increases the strength but also the toughness of CF reinforced composites. For 0.5 wt%–NH_2–PPTA/CF/epoxy, σ_f and ILSS are increased by ~16% and ~27%, respectively. Because flexural properties of continuous CF reinforced polymers is mainly determined by CFs, NH_2-PPTA can only slightly improve the flexural strength. However, as shown in Table S4, NH_2-PPTA increases ILSS more effectively than some previously reported MWCNTs and carbon nanofibers. Moreover, addition of NH_2-PPTA leads to an increase of E_{tot} by ~67%, indicating that NH_2-PPTA is effective for increasing the toughness of CF/epoxy composites, which is of great significance for the application of CF/epoxy composites. At higher NH_2-PPTA contents, the reinforcement becomes less effective. This may be related to the high viscosity of NH_2-PPTA/epoxy with a high NH_2-PPTA content, which makes it difficult for the resin to wet the carbon fibers sufficiently during the preparation of the CF/NH_2-PPTA/epoxy composites.

4. Conclusions

Aminated aromatic polyamide NH_2-PPTA was prepared by low-temperature solution polycondensation followed by hydrogenation reduction. The rigid-rod NH_2-PPTA is demonstrated to be idea reinforcing and toughening agent of epoxy resin. When the NH_2-PPTA content is less than 0.5 wt%, NH_2-PPTA is dispersed at the molecular level in the epoxy resin, and when the NH_2-PPTA content is higher, the molecular composite is converted into a nanocomposite due to microphase separation and the formation of nanorod- or nanofiber-like aggregates in the matrices.

NH_2-PPTA improves both the strength and toughness of epoxy resin. A maximum tensile strength of 100.7 ± 5.3 MPa was achieved for 0.7 wt %–NH_2–PPTA/epoxy, which is increased by ~74% compared with that of neat epoxy resin. Furthermore, the elongation at break and tensile toughness are improved by ~30% and ~131%, respectively, for 1.3 wt %–NH_2–PPTA/epoxy. The flexural strength is also improved to 179.2 ± 0.9 MPa for 0.9 wt%–NH_2–PPTA/epoxy, which is increased by ~41%. The flexural toughness and the notched Izod impact strength are increased by ~143% and ~14%, respectively. Moreover, NH_2-PPTA is also found to be effective for the modification of CF/epoxy composites. For 0.5 wt%–NH_2–PPTA/CF/epoxy composite, the flexural strength, ILSS and E_{tot} are increased by ~16%, ~27% and ~67%, respectively. Preparation of NH_2-PPTA/epoxy composites is relatively convenient, and the reinforcing effect of NH_2-PPTA is even better than many previously reported carbonaceous and inorganic nanofillers. Therefore, NH_2-PPTA can be used in many high performance thermosetting composites and CFRPs in place of or in combination with traditional nanomaterials in the future.

Declaration of competing interest

The authors declare that they have no known competing financial interests or personal relationships that could have appeared to influence

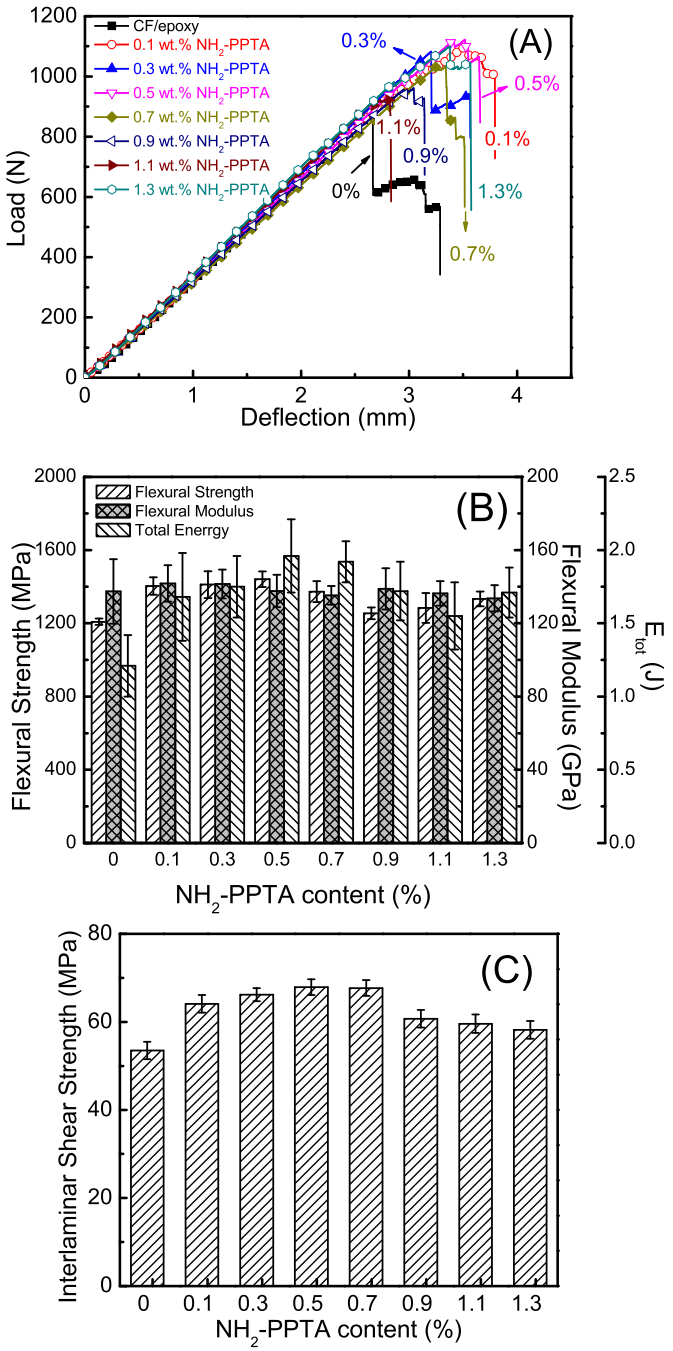

Fig. 10. (A) Load-deflection curves of CF/epoxy and CF/NH_2-PPTA/epoxy composites and the histograms of (B) the flexural properties and (C) ILSS.

the work reported in this paper.

CRediT authorship contribution statement

Boshi Yu: Validation, Writing - review & editing.

Acknowledgment

Financial support from the National Natural Science Foundation of China (51973182 and 51573164) is acknowledged.

Appendix A. Supplementary data

Supplementary data to this article can be found online at https://doi.org/10.1016/j.compositesb.2020.108044.

References

[1] Arnold Jr F, Arnold FE. Rigid-rod polymers and molecular composites. In: Hergenrother P, editor. High performance polymers. Springer Berlin Heidelberg; 1994. p. 257–95.
[2] Hwang W, Wiff D, Benner C, Helminiak T. Composites on a molecular level: phase relationships, processing, and properites. J Macromol Sci, Part B: Physics 1983;22 (2):231–57.
[3] Akita H, Kobayashi H, Hattori T, Kagawa K. Studies on molecular composite. II. Processing of molecular composites using copolymers consisting of a precursor of poly(p-phenylene benzobisthiazole) and aromatic polyamide. J Polym Sci B Polym Phys 1999;37(3):199–207.
[4] Takayanagi M, Ogata T, Morikawa M, Kai T. Macromol. Sci. Phys. 1980;B17(4): 591.
[5] Flory PJ, Abe A. Statistical thermodynamics of mixtures of rodlike particles. 1. Theory for polydisperse systems. Macromolecules 1978;11(6):1119–22.
[6] Tsou L, Sauer J, Hara M. Mechanical properties of molecular composites. I. Poly (p-phenylene terephthalamide) anion molecules dispersed in poly (4-vinylpyridine). J Polym Sci B Polym Phys 1999;37(16):2201–9.
[7] Tsou L, Sauer JA, Hara M. Molecular composites of poly(p-phenylene terephthalamide) anion and poly(propylene oxide): mechanical properties. Polymer 2000;41(22):8103–11.
[8] Chen WC, Sauer JA, Hara M. Molecular composites made of ionic poly(p-phenylene terephthalamide) and poly(4-vinylpyridine): relaxation behavior. J Polym Sci B Polym Phys 2002;40(11):1110–7.
[9] Venkatasubramanian N, Dean DR, Dang TD, Price GE, Arnold FE. Solvent cast thermoplastic and thermoset rigid-rod molecular composites. Polymer 2000;41(9): 3213–26.
[10] Winter D, Eisenbach CD. Poly(arylene-ethynylene) with tuned rigidity/flexibility as reinforcing component in polystyrene-based ionomer blends. Polymer 2004;45 (8):2507–15.
[11] Bayer A, Datko A, Eisenbach CD. Interactions and mechanical properties of rod–coil ionomer blend. Polymer 2005;46(17):6614–22.
[12] Cowie JMG, Nakata S, Adams GW. Blends of some non-flexible and flexible polymers: routes to molecular composites? Macromol Symp 1996;112(1):207–16.
[13] Mehta R, Dadmun MD. Small angle neutron scattering studies on miscible blends of poly(styrene-ran-vinyl phenol) with liquid crystalline polyurethane. Macromolecules 2006;39(25):8799–807.
[14] Peng M, Xiao G, Tang X, Zhou Y. Hydrogen-bonding assembly of rigid-rod poly(p-sulfophenylene terephthalamide) and flexible-chain poly(vinyl alcohol) for transparent, strong, and tough molecular composites. Macromolecules 2014;47 (23):8411–9.
[15] Koo B, Subramanian N, Chattopadhyay A. Molecular dynamics study of brittle fracture in epoxy-based thermoset polymer. Compos B Eng 2016;95:433–9.
[16] Sharma S, Singh BP, Chauhan SS, Jyoti J, Arya AK, Dhakate SR, et al. Enhanced thermomechanical and electrical properties of multiwalled carbon nanotube paper reinforced epoxy laminar composites. Compos Appl Sci Manuf 2018;104 (Supplement C):129–38.
[17] Dahmen V, Redmann AJ, Austermann J, Quintanilla AL, Mecham SJ, Osswald TA. Fabrication of hybrid composite T-joints by co-curing with 3D printed dual cure epoxy. Compos B Eng 2020:183.
[18] Yang X, Zhu J, Yang D, Zhang J, Guo Y, Zhong X, et al. High-efficiency improvement of thermal conductivities for epoxy composites from synthesized liquid crystal epoxy followed by doping BN fillers. Compos B Eng 2020:185.
[19] Ionita M. Multiscale molecular modeling of SWCNTs/epoxy resin composites mechanical behaviour. Compos B Eng 2012;43(8):3491–6.
[20] Li Y, Wang S, Wang Q, Xing M. A comparison study on mechanical properties of polymer composites reinforced by carbon nanotubes and graphene sheet. Compos B Eng 2018;133:35–41.
[21] Zakaria MR, Md Akil H, Abdul Kudus MH, Ullah F, Javed F, Nosbi N. Hybrid carbon fiber-carbon nanotubes reinforced polymer composites: a review. Compos B Eng 2019;176:107313.
[22] Cha J, Kim J, Ryu S, Hong SH. Strengthening effect of melamine functionalized low-dimension carbon at fiber reinforced polymer composites and their interlaminar shear behavior. Compos B Eng 2019:173.
[23] Yao X, Gao X, Jiang J, Xu C, Deng C, Wang J. Comparison of carbon nanotubes and graphene oxide coated carbon fiber for improving the interfacial properties of carbon fiber/epoxy composites. Compos B Eng 2018;132:170–7.
[24] Zakaria MR, Akil HM, Kudus MHA, Ullah F, Javed F, Nosbi N. Hybrid carbon fiber-carbon nanotubes reinforced polymer composites: a review. Compos B Eng 2019: 176.
[25] Li Y, Hori N, Arai M, Hu N, Liu Y, Fukunaga H. Improvement of interlaminar mechanical properties of CFRP laminates using VGCF. Compos Appl Sci Manuf 2009;40(12):2004–12.
[26] Hu N, Li Y, Nakamura T, Katsumata T, Koshikawa T, Arai M. Reinforcement effects of MWCNT and VGCF in bulk composites and interlayer of CFRP laminates. Compos B Eng 2012;43(1):3–9.
[27] Khan SU, Munir A, Hussain R, Kim J-K. Fatigue damage behaviors of carbon fiber-reinforced epoxy composites containing nanoclay. Compos Sci Technol 2010;70 (14):2077–85.
[28] Peng M, Zhou Y, Zhou G, Yao H. Triglycidyl para-aminophenol modified montmorillonites for epoxy nanocomposites and multi-scale carbon fiber

reinforced composites with superior mechanical properties. Compos Sci Technol 2017;148:80–8.
[29] Zabihi O, Ahmadi M, Nikafshar S, Chandrakumar Preyeswary K, Naebe M. A technical review on epoxy-clay nanocomposites: structure, properties, and their applications in fiber reinforced composites. Compos B Eng 2018;135:1–24.
[30] Yao HC, Zhou GD, Wang WT, Peng M. Effect of polymer-grafted carbon nanofibers and nanotubes on the interlaminar shear strength and flexural strength of carbon fiber/epoxy multiscale composites. Compos Struct 2018;195:288–96.
[31] Yao HC, Zhou GD, Wang WT, Peng M. Silica nanoparticle-decorated alumina rough platelets for effective reinforcement of epoxy and hierarchical carbon fiber/epoxy composites. Compos Appl Sci Manuf 2018;110:53–61.
[32] Peng M, Tang X, Zhou Y. Fast phase transfer of graphene oxide from water to triglycidyl para-aminophenol for epoxy composites with superior nanosheet dispersion. Polymer 2016;93:1–8.
[33] Chandra Y, Scarpa F, Adhikari S, Zhang J, Saavedra Flores EI, Peng H-X. Pullout strength of graphene and carbon nanotube/epoxy composites. Compos B Eng 2016;102:1–8.
[34] Adak NC, Chhetri S, Murmu NC, Samanta P, Kuila T, Lee JH. Experimental and numerical investigation on the mechanical characteristics of polyethylenimine functionalized graphene oxide incorporated woven carbon fibre/epoxy composites. Compos B Eng 2019;156:240–51.
[35] Ioniţă M, Vlăsceanu GM, Watzlawek AA, Voicu SI, Burns JS, Iovu H. Graphene and functionalized graphene: extraordinary prospects for nanobiocomposite materials. Compos B Eng 2017;121:34–57.
[36] Tang XL, Zhou Y, Peng M. Green preparation of epoxy/graphene oxide nanocomposites using a glycidylamine epoxy resin as the surface modifier and phase transfer agent of graphene oxide. ACS Appl Mater Interfaces 2016;8(3):1854–66.
[37] Khan NI, Haider S, Das S, Wang J. Exfoliation level of aggregated graphitic nanoplatelets by oxidation followed by silanization on controlling mechanical and nanomechanical performance of hybrid CFRP composites. Compos B Eng 2019:173.
[38] Ma L, Zhu Y, Feng P, Song G, Huang Y, Liu H, et al. Reinforcing carbon fiber epoxy composites with triazine derivatives functionalized graphene oxide modified sizing agent. Compos B Eng 2019:176.
[39] Pawlik M, Le H, Lu Y. Effects of the graphene nanoplatelets reinforced interphase on mechanical properties of carbon fibre reinforced polymer - a multiscale modelling study. Compos B Eng 2019:177.
[40] Xu Z, Song P, Zhang J, Guo Q, Mai Y-W. Epoxy nanocomposites simultaneously strengthened and toughened by hybridization with graphene oxide and block ionomer. Compos Sci Technol 2018;168:363–70.
[41] Liu S, Chevali VS, Xu Z, Hui D, Wang H. A review of extending performance of epoxy resins using carbon nanomaterials. Compos B Eng 2018;136:197–214.
[42] Herring ML, Fox BL. The effect of a rapid curing process on the surface finish of a carbon fibre epoxy composite. Compos B Eng 2011;42(5):1035–43.
[43] Hu N, Li Y, Nakamura T, Katsumata T, Koshikawa T, Arai M. Reinforcement effects of MWCNT and VGCF in bulk composites and interlayer of CFRP laminates. Compos B Eng 2012;43(1):3–9.
[44] Kim H. Enhanced crack detection sensitivity of carbon fiber composites by carbon nanotubes directly grown on carbon fibers. Compos B Eng 2014;60:284–91.
[45] Ning HM, Weng SY, Hu N, Yan C, Liu J, Yao JY, et al. Mode-II interlaminar fracture toughness of GFRP/Al laminates improved by surface modified VGCF interleaves. Compos B Eng 2017;114:365–72.
[46] Storck S, Malecki H, Shah T, Zupan M. Improvements in interlaminar strength: a carbon nanotube approach. Compos B Eng 2011;42(6):1508–16.
[47] Xiong CY, Li TH, Zhao TK, Dang AL, Li H, Ji XL, et al. Reduced graphene oxide-carbon nanotube grown on carbon fiber as binder-free electrode for flexible high-performance fiber supercapacitors. Compos B Eng 2017;116:7–15.
[48] Zhang LM, De Greef N, Kalinka G, Van Bilzen B, Locquet JP, Verpoest I, et al. Carbon nanotube-grafted carbon fiber polymer composites: damage characterization on the micro-scale. Compos B Eng 2017;126:202–10.
[49] Nistal A, Falzon BG, Hawkins SC, Chitwan R, García-Diego C, Rubio F. Enhancing the fracture toughness of hierarchical composites through amino–functionalised carbon nanotube webs. Compos B Eng 2019;165:537–44.
[50] Liu C, Dong YF, Lin Y, Yan HX, Zhang WB, Bao Y, et al. Enhanced mechanical and tribological properties of graphene/bismaleimide composites by using reduced graphene oxide with non-covalent functionalization. Compos B Eng 2019;165:491–9.
[51] Ma LC, Zhu YY, Feng PF, Song GJ, Huang YD, Liu H, et al. Reinforcing carbon fiber epoxy composites with triazine derivatives functionalized graphene oxide modified sizing agent. Compos B Eng 2019:176.
[52] Mishra K, Singh RP. Effect of APTMS modification on multiwall carbon nanotube reinforced epoxy nanocomposites. Compos B Eng 2019;162:425–32.
[53] Higashi F, Nishi T. High-molecular-weight poly(p-phenyleneterephthalamide) by CaCl2 promoted direct polycondensation with thionyl chloride in N-methylpyrrolidone. J Polym Sci Polym Chem 1988;26(12):3235–40.
[54] Esteves ACC, Barros-Timmons AM, Martins JA, Zhang W, Cruz-Pinto J, Trindade T. Crystallization behaviour of new poly(tetramethyleneterephthalamide) nanocomposites containing SiO2 fillers with distinct morphologies. Compos B Eng 2005;36(1):51–9.
[55] Liu Z, Zhang J, Tang L, Zhou Y, Lin Y, Wang R, et al. Improved wave-transparent performances and enhanced mechanical properties for fluoride-containing PBO precursor modified cyanate ester resins and their PBO fibers/cyanate ester composites. Compos B Eng 2019;178:107466.
[56] Chao D, Lu X, Chen J, Liu X, Zhang W, Wei Y. Synthesis and characterization of electroactive polyamide with amine-capped aniline pentamer and ferrocene in the main chain by oxidative coupling polymerization. Polymer 2006;47(8):2643–8.
[57] Cretenoud J, Ozen B, Schmaltz T, Gorl D, Fabrizio A, Corminboeuf C, et al. Synthesis and characterization of semiaromatic polyamides comprising benzofurobenzofuran repeating units. Polym Chem 2017;8(14):2197–209.
[58] Nimita Jebaranjitham J, Mageshwari C, Saravanan R, Mu N. Fabrication of amine functionalized graphene oxide – AgNPs nanocomposite with improved dispersibility for reduction of 4-nitrophenol. Compos B Eng 2019;171:302–9.
[59] Jovanović V, Samaržija-Jovanović S, Dekić B, Dekić V, Konstaninović S, Marković G, et al. Effect of γ-irradiation on the thermo-oxidative behavior of nano-silica based urea–formaldehyde hybrid composite with 4-chloro-3-nitro-2H-chromen-2-one. Compos B Eng 2013;45(1):864–70.
[60] Leibler L. Theory of microphase separation in block copolymers. Macromolecules 1980;13(6):1602–17.
[61] Zhang Y, Shi W, Chen F, Han CC. Dynamically asymmetric phase separation and morphological structure formation in the epoxy/polysulfone blends. Macromolecules 2011;44(18):7465–72.
[62] Peng M, Li DS, Chen Y, Zheng Q. Effect of an organoclay on the reaction-induced phase-separation kinetics and morphology of a poly(ether imide)/epoxy mixture. J Appl Polym Sci 2007;104(2):1205–14.
[63] Tan L-S, Arnold FE. Ionically blended molecular composites. Google Patents; 1992.
[64] Li P, Zheng Y, Shi T, Wang Y, Li M, Chen C, et al. A solvent-free graphene oxide nanoribbon colloid as filler phase for epoxy-matrix composites with enhanced mechanical, thermal and tribological performance. Carbon 2016;96:40–8.
[65] Peng M, Tang XL, Zhou Y. Fast phase transfer of graphene oxide from water to triglycidyl para-aminophenol for epoxy composites with superior nanosheet dispersion. Polymer 2016;93:1–8.
[66] Ming-Yuan H, Hutchinson JW. Crack deflection at an interface between dissimilar elastic materials. Int J Solid Struct 1989;25(9):1053–67.
[67] Schartel B, Wendorff JH. Molecular composites for molecular reinforcement: a promising concept between success and failure. Polym Eng Sci 1999;39(1):128–51.
[68] Bekyarova E, Thostenson ET, Yu A, Kim H, Gao J, Tang J, et al. Multiscale carbon Nanotube−Carbon fiber reinforcement for advanced epoxy composites. Langmuir 2007;23(7):3970–4.
[69] Zhou G, Yao H, Zhou Y, Wang W, Peng M. Self-assembled complexes of graphene oxide and oxidized vapor-grown carbon fibers for simultaneously enhancing the strength and toughness of epoxy and multi-scale carbon fiber/epoxy composites. Carbon 2018;137:6–18.
[70] Park S-J, Seo M-K, Lee D-R. Studies on the mechanical and mechanical interfacial properties of carbon–carbon composites impregnated with an oxidation inhibitor. Carbon 2003;41(15):2991–3002.